Automatic Identification of CTC in Fluorescence Microscopy Images Based on A Lightweight Hybrid Network Model

Kazuki Nakamichi [1], Kouki Tsuji [1], Kazue Yoneda [2,3], and Tohru Kamiya [1,*]

[1] Department of Mechanical and Control Engineering, Kyushu Institute of Technology, 1-1, Sensui, Tobata, Kitakyushu 804-8550, Japan
[2] Department of Thoracic Oncology, School of Medicine, Hyogo Medical University, 1-1, Mukogawa-cho, Nishinomiya, Hyogo 663-8501, Japan
[3] Second Department of Surgery (Chest Surgery), University of Occupational and Environmental Health, 1-1, Iseigaoka, Yahatanishi, Kitakyushu 807-8555, Japan
Email: tsuji.kouki550@mail.kyutech.jp (K.T.); kyoneda@hyo-med.ac.jp (K.Y.); kamiya@cntl.kyutech.ac.jp (T.K.)
*Corresponding author

***Abstract*—Circulating Tumor Cells (CTC) are expected to be a useful biomarker for cancer metastasis. CTC analysis can be used to assess cancer status and the therapeutic effects of anticancer drugs. Pathologists analyze blood samples from images taken with a fluorescence microscope. However, the number of CTCs in blood is very small, which is a time-consuming task. In this paper, we propose an automatic CTC identification method from fluorescence microscopy images. In the proposed method, we detect cell regions using a selective enhancement filter and blob analysis. Then, we identify the CTC using a SqueezeNet-based Convolutional Neural Network (CNN) model with Spatial Pyramid Pooling (SPP). We apply the proposed method to 5040 microscopy images and evaluate its effectiveness. The experimental results show that the proposed method has a true positive rate of 97.30%, a false positive rate of 2.069%, and an Area Under the Curve (AUC) of 0.991.**

***Keywords*—Circulating Tumor Cells (CTC), fluorescence microscopy images, SqueezeNet, Spatial Pyramid Pooling (SPP)**

I. Introduction

Circulating Tumor Cells are expected to be a useful biomarker for cancer metastasis [1]. CTC are cells that have been shed from a primary tumor and circulate in the blood of patients. CTC can spread to distant sites in the body and may generate new cancer in other organs. Analysis of these CTC is expected to enable early detection of cancer and evaluation of the therapeutic effects of anticancer drugs. There are various devices for CTC analysis, however, research on the universal CTC chip has been advanced as a tool that can detect CTC with high accuracy [2, 3]. This chip is a polymer microfluidic device to capture the CTCs. There are more than 30,000 microposts in a channel on the surface of the CTC chip body. These microposts can be coated with any antibody and can capture various cells in the blood. In this paper, we use three kinds of fluorescence reactions to identify CTC. Table I shows the fluorescence reaction pattern of CTC. In the table, "+" indicates a positive reaction and "–" indicates a negative reaction. Here, cytokeratin reacts to red light, leukocyte reacts to green light, and nucleus reacts to blue light. In this paper, we used Leica DMi8 inverted microscope [4] for fluorescence emission and imaging of cells.

Pathologists detect cells with the characteristics shown in Table I from the three types of captured images. However, it is laborious and time-consuming for pathologists because the number of CTCs contained in blood is very small. In addition, there is a problem that identification depends on the subjectivity of the pathologists. Therefore, the development of a quantitative automatic CTC identification method by computer is required in medical fields. Other problems include manual identification, low numbers of CTCs, and the possibility of operating error. In general, there are no publicly available data sets for the training and testing of the identification of the CTC.

In our previous study, Tsuji *et al*. [5] proposed two types of automatic CTC detection methods: logical combination of cell regions and Artificial Neural Network (ANN). The proposed method is divided into two steps: cell region detection and CTC identification. First, cell regions are mainly detected by filtering methods. Then, in the logical conjunction method, segmentation was applied to the Region of Interest (ROI) cut out from the three-color images, and those that satisfied the results in Table I were identified as CTCs. In the method using ANN, they compute feature values from each ROI and identify CTC using ANN classifier. However, these methods have problems in versatility because the segmentation method and the selection of

Manuscript received December 19, 2024; revised January 23, 2025; accepted March 6, 2025; published May 9, 2025.

features depend on the algorithms. Also, many cellular regions are represented in an image, especially when multiple cells are connected, and there are many cases where accurate segmentation is difficult to achieve in image processing. The current state of image processing technology does not provide a method for separating individual multicellular regions, and improvements in this area are needed.

TABLE I. THE REACTION OF CTC

	Cytokeratin	Leukocyte	Cell nucleus
Reaction	+	–	+

Recently, Convolutional Neural Network has attracted attention in the field of image recognition. CNN is a method that can automatically extract features effective for identification from images and has been shown to be very useful in various pattern recognition fields. In addition, Mao *et al.* [6] proposed a method for detecting CTC using CNN from images taken with a phase contrast microscope and demonstrated that the method provided superior results compared to the detection method using manually selected features. Therefore, in this paper, we propose a CTC identification method using a CNN model based on SqueezeNet [7] with Spatial Pyramid Pooling (SPP) [8]. Spatial pyramid pooling is one of the most successful methods in computer vision. It divides the image into subdivisions from finer to coarser levels and aggregates local features in these subdivisions. SPP has long been a key component in leading and award-winning classification and detection systems, even before the recent proliferation of CNNs. In this paper, we introduced SPP to extract local features and spatial variability on CTCc in microscopy images.

II. METHODS

We capture the specific cells from the blood sample (1 mL) using the Universal CTC Chip. This sample is generated by adding the cancer cell line to healthy human blood. The three types of targets shown in Table I are reacted, and microscopy images are generated by DMi8. Fig. 1 shows an example of the generated image.

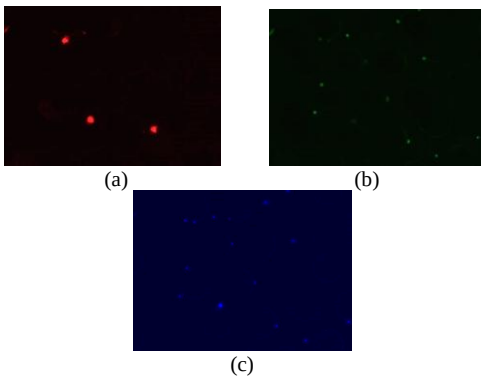

Fig. 1. Example of fluorescence microscopy images; Three images are parts of the original image that have been cropped to improve visibility and further processed, such as contrast enhancement. (a) Red image (cytokeratin); (b) Green image (leukocyte); (c) Blue image (cell nucleus).

The three images shown in Fig. 1 are parts of the original image that have been cropped to improve visibility and further processed, such as contrast enhancement. In this paper, we propose a method to automatically identify CTC using these three colors of images. Our proposed method consists of two steps: "cell region detection" and "CTC identification". First, we detect cell regions from red images. Then, we set the ROI for red, green and blue images, respectively, using the coordinated information of the cells extracted from the red image. Finally, we identify the CTC using the three extracted ROI. The details are described below.

A. Detection of Cell Regions

As described above, microscopy images have three channels. Three types of images are taken at the same coordinate on the CTC chip, so objects located at the same position of three images correspond to each other. Therefore, we first detect cell regions on red images, and we cut out ROI from each image using the detection results. The reason why red images are used here is that red cells are clearer, and the number of cells is smaller than other channels on the image. Typically, in CTC analysis, pathologists first search for cell regions in red images and then refer to the same coordinates in blue and green images.

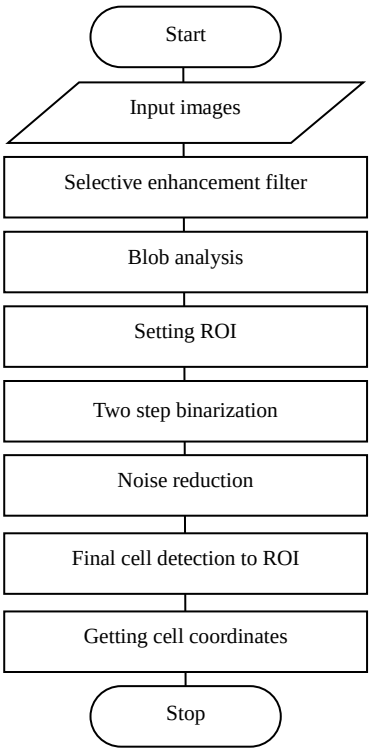

Fig. 2. Flow of the cell detection.

Fig. 2 shows the detection process. First, we highlight cell regions using the selective enhancement filter [9]. The selective enhancement filter is a filter algorithm based on Hessian matrix analysis that can selectively enhance point or line components in images. The selective enhancement filter is mainly designed to detect lesions in medical images and can selectively coordinate

the round shape of nodular shadows and the elongated feature of blood vessels based on the eigenvalue analysis of the Hesse matrix. As a result, blood vessels and round shadows can be selectively removed or retained from an image. When separating CTCs, it is possible to efficiently separate cellular regions other than those appearing in the image background. In this paper, since the shape of the cell regions is almost circular, a filter that emphasizes the point components is applied. The minimum diameter to be emphasized is 9, the maximum diameter is 33, and the smoothing scale is $N = 5$. This filter is also used in our previous method of Tsuji *et al*. [5].

Next, we binarize the highlight result by using multiple thresholds and perform blob analysis [10]. The blob analysis is a process to analyze the features of labeled regions on a binary image. In this paper, four types of features are used: area, circularity, inertia ratio, and convexity. We binarize images by using ten thresholds, and the region where satisfaction with four kinds of feature values by five or more images is detected as the cell candidate region. By this processing, it is possible to detect the cell regions that show the shape stable over different thresholds on the grayscale image. In this paper, the range of the condition of the feature is experimentally set as an area: 40 to 400 pixels, circularity: 0.6 to 1.0, inertia ratio: 0.3 to 1.0, and convexity: 0.7 to 1.0. After that, we set a ROI of 64×64 pixels around the detected region.

Finally, we perform the detection of cell regions in the ROI. We perform a two-step binarization on the ROI. In this method, binarization is performed by the discriminant analysis method [11], and binarization is performed again by the discriminant analysis method using only the pixel values in the region that exceed the threshold of the first binarization. Through this processing, it is possible to detect even cell regions that have a pale color. Finally, noise reduction is applied to the binary image. In this work, the region of the binary image whose area is 10 or less, 400 or more, or whose circularity is 0.5 or less is removed as a noise component. After that, the remaining area is considered as cell regions, and we obtain its coordinates. Using the coordinates obtained here, a ROI of 32×32 pixels is extracted from each of the red, green and blue images.

B. Identification of CTC

1) Generation of input images to CNN

The RGB color image created by combining the extracted three-color images is used as input. The example of input images is shown in Fig. 3. In Fig. 3, (1) is a CTC that satisfies the conditions in Table I, and (2) is a normal cell because it only responds to red. In this paper, the data set is biased because the number of CTC data is very small. Therefore, we propose a data augmentation method that changes the combination of red and blue images of CTC data. Normally, three ROI cut from the same coordinates are combined, but we create pseudo-CTC data by combining ROI of cytokeratin (red) and nucleus (blue) cut from different coordinates. These images are used as training data. For example, if three types of images cut from the same coordinates are R-1, G-1, and B-1, we combine R-1 and G-1 with B-2 and B-3 cut from different coordinates. As shown in Table I, CTC is a cell that has no response on the green image and responses on the red and blue images. Therefore, even though it is not a combination of cells at the same coordinate, it is assumed that pseudo-CTC data can be generated by combining three color images at different coordinates to satisfy this condition.

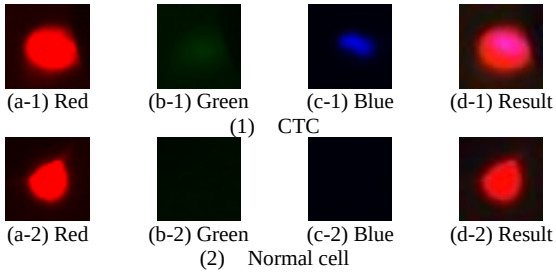

Fig. 3. Generation of input images to CNN: Top row shows a CTC that satisfies the conditions in Table I, and bottom row shows a normal cell because it only responds to red.

2) CTC identification by CNN

In this paper, we propose a CNN model based on SqueezeNet [7] with SPP [8]. SqueezeNet is a model that achieves high accuracy with a small number of parameters. The SqueezeNet achieves AlexNet-level accuracy on ImageNet with 50x fewer parameters. Additionally, with model compression techniques able to compress SqueezeNet to less than 0.5 MB (510x smaller than AlexNet). We adopted this lightweight model, which can perform learning efficiently with few parameters, because the size of the input images is small, and our goal of identification is only two classes. As a feature of SqueezeNet, there is a structure called “fire module” as shown in Fig. 4. The fire module consists of “squeeze” layers, which consist of 1×1 convolutional layers, and “expand” layers, which consist of 1×1 and 3×3 convolutional layers. The dimension of the feature map is reduced in the squeeze layer and restored as the features are extracted in the expand layer.

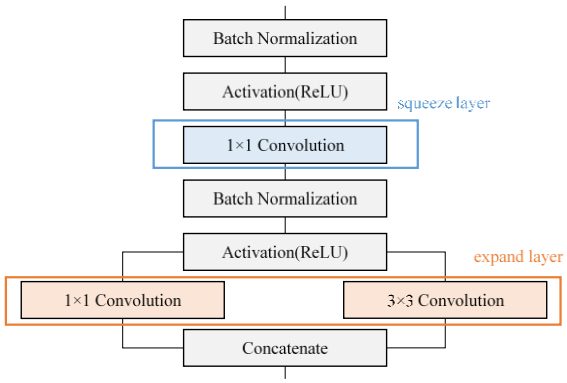

Fig. 4. Detail of Fire module: The fire module consists of “squeeze” layers, and “expand” layers.

SPP is a kind of pooling layer. Fig. 5 shows the details of the SPP. The SPP is a layer that divides the feature map of the input into a fixed number of regions and outputs

the result of maximum pooling for each region. Since it outputs information from multiple divided regions, it is possible to extract global and local features at the same time. The output feature vector is used as the input of the fully connected layer to identify the object.

Fig. 6 shows the CNN model of the proposed method. In Fig. 6, BN means batch normalization. In the proposed method, the part where Global Average Pooling (GAP) was used in the original SqueezeNet is changed to SPP. GAP is a pooling method that outputs the average value of all channels in the feature map. It is possible to extract more detailed features by changing to SPP.

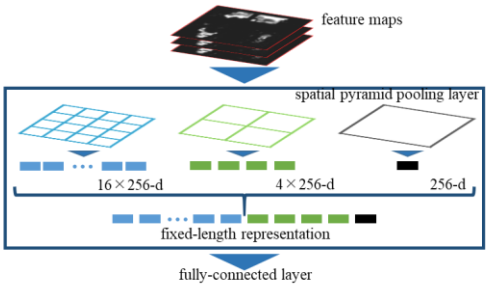

Fig. 5. Detail of SPP: The SPP is a layer that divides the feature map and outputs the result of maximum pooling for each region.

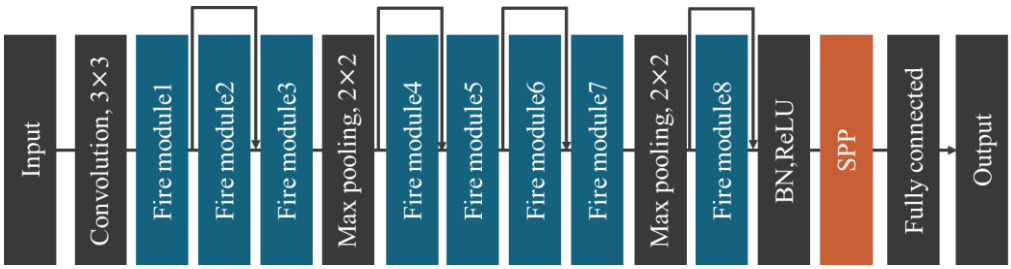

Fig. 6. The network architecture of proposed model: BN shows batch normalization. GAP in SqueezeNet is changed to SPP.

C. Comparison with Other Methods

To demonstrate the usefulness of the proposed method, we perform two comparative experiments: CNN model and data augmentation method. For the CNN model, we perform CTC identification experiments using AlexNet [12] and Residual Network (ResNet) [13] in addition to SqueezeNet. AlexNet is a model consisting of five convolutional layers, two pooling layers, and three fully connected layers. ResNet is a model in which gradient vanishing is unlikely to occur even as the number of layers increases due to the introduction of short-cut connections. In this paper, we used a model consisting of one convolutional layer, five residual block layers, one global average pooling layer, and one fully connected layer.

About the augmentation method, we perform the experiment using Mixup [14]. Mixup is a method to combine any two-training data and create new data. Mixup is a technique to increase data diversity through the mixing of training data, which can be effective in improving the generalization performance of the model. Specifically, assuming that the two-image data are x_1 and x_2, and the labels corresponding to the images are y_1 and y_2, new image data x and label y are created using the following equation.

$$x = \lambda x_1 + (1-\lambda)x_2 \tag{1}$$

$$y = \lambda y_1 + (1-\lambda)y_2 \tag{2}$$

λ is the composite ratio sampled from the beta distribution *Beta (α, α)*. In this paper, we use α = 0.2 experimentally and apply Mixup to only CTC data to obtain training data. Fig. 7 shows an example of images generated by Mixup.

Fig. 7. Example of Mixup: Increase data diversity through the mixing of training data.

III. Experimental Results

We applied the proposed method to 5040 fluorescence microscopy images (6 samples). Sample 1 and 4 contain 810 images, and the other 4 samples contain 855 images each. Again, these image sizes are 1296×966 pixels. The learning of the CNN model used for identification was optimized using Adaptive Moment Estimation (Adam). In terms of hyperparameters, the learning rate is 0.01, the batch size is 128, and the maximum number of iterations is 20,000. To reduce overfitting due to lack of data, data augmentation was performed using the proposed method or Mixup for CTC data. For normal cell images, data augmentation was performed by randomly applying rotation, vertical flip, horizontal flip, width shift, and height shift.

We calculated the accuracy of CTC identification using True Positive Rate (TPR), False Positive Rate (FPR), and Area Under the Curve (AUC) based on Receiver Operating Characteristics (ROC) curve. TPR and FPR are defined in the following equation:

$$TPR = \left\{\frac{a}{a+b}\right\} \times 100 \tag{3}$$

$$FPR = \left\{\frac{c}{c+d}\right\} \times 100 \tag{4}$$

where *a*, *b*, *c* and *d* are shown in the confusion matrix in Table II. In this table, ground truth is the correct data of CTC contained in each sample, and it was manually generated by pathologists. In this paper, ground truth is used as the correct response data for performance evaluation. In addition, positive indicates CTC and negative indicates non-CTC. The ROC curve shows the relationship between TPR and FPR. AUC indicates the area under the ROC curve, and the closer the value is to 1, the better the model performance. The average identification performance of the proposed method was evaluated using the leave-one-out cross-validation method. Table III shows the identification results and Fig. 8 shows the ROC curve. As a result, the TPR of 97.30%, the FPR of 2.069% and the AUC of 0.991 were obtained, respectively.

TABLE II. CONFUSION MATRIX

		Ground truth	
		Positive	**Negative**
Identification result by our method	**Positive**	*a*	*c*
	Negative	*b*	*d*

TABLE III. IDENTIFICATION RESULT OF THE PROPOSED METHOD

Sample	TPR [%]	FPR [%]	AUC
1	100.0	0.891	0.998
2	92.31	1.613	0.994
3	97.06	2.590	0.989
4	100.0	1.856	0.997
5	100.0	5.195	0.985
6	97.72	2.492	0.994
Average	**97.30**	**2.069**	**0.991**

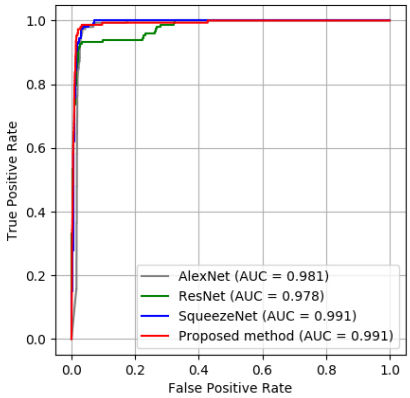

Fig. 8. ROC curve of each CNN models: Propose method obtained best performance based on ROC.

Table IV shows the average results of identification by using another CNN model, and Fig. 8 shows the ROC curve. From these results, it was confirmed that the proposed CNN model showed better results than other methods. Table V shows the average identification result of three CNN models using the training data augmented by Mixup, and Fig. 9 shows the ROC curve. There was no significant difference between the proposed data augmentation and Mixup.

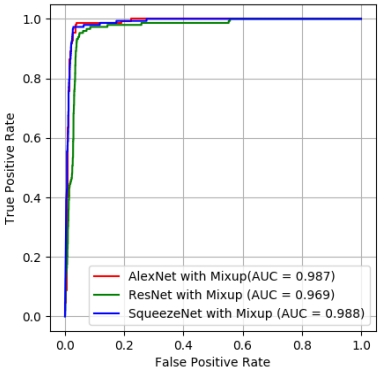

Fig. 9. ROC curve of Mixup.

TABLE IV. IDENTIFICATION RESULTS OF EACH CNN MODEL

Proposed Model	TPR [%]	FPR [%]	AUC
SqueezeNet [7]	97.30	3.150	0.991
AlexNet [12]	97.30	3.459	0.981
ResNet [13]	93.24	4.20	0.978

TABLE V. IDENTIFICATION RESULTS OF EACH CNN MODEL USING MIXUP

Proposed Model	TPR [%]	FPR [%]	AUC
SqueezeNet [7]	97.30	2.996	0.988
AlexNet [12]	97.30	3.706	0.987
ResNet [13]	93.24	4.324	0.969

In addition, the experimental results in the case of automatic CTC identification using the method of Tsuji *et al.* [5] are shown in Table VI. From the above, our proposed CNN model improves the TPR and FPR compared to the method of Tsuji *et al.* On the other hand, the computation time for segmentation and CTC identification is a few seconds on a PC with an IntelCorei7 CPU with 8 GB GPU Memory. There is no difference in computation time compared to other comparison methods.

TABLE VI. IDENTIFICATION RESULTS OF PREVIOUS STUDY [5]

Methods	TPR [%]	FPR [%]
Logical conjunction	95.27	6.172
ANN	93.24	8.003

IV. DISCUSSIONS

In this paper, we proposed an automatic CTC identification method in fluorescence microscopy images based on CNN. The results of the performance evaluation are discussed below.

From Tables III and IV, the proposed method showed the best results among the four models tested. This is because the fire module, the unique structure of SqueezeNet was able to efficiently capture the characteristics of CTC. In addition, the introduction of SPP enables the global and local features to be extracted collectively, which also contributes to the improvement of accuracy. In the original SqueezeNet, as shown in Fig. 10, some images that did not show the shape of the cell, although the reaction pattern in Table I was satisfied,

were sometimes misidentified as CTC. However, by introducing the SPP, it was possible to capture the fine features of the shape so that the misidentification as shown in Fig. 8 was reduced, resulting in the improvement of the FPR.

Fig. 10. Example of false positive when we used the original model.

From Tables IV and V, comparing the proposed data enhancement method that recombines RGB data with Mixup, there was no significant difference. Here, Fig. 9 shows the distribution of each identification result in SqueezeNet. In Fig. 9, the legend in the bottom center shows the probability of CTC. The closer this value is to 1, the more the classifier determines that the input image is likely to be a CTC. The variability of the likelihood is higher when using Mixup than when using the proposed method. This is probably since Mixup performs the process of mixing two images, which weakens the features of CTC. Because Mixup mixes two images while diluting them, it can produce CTC data with a weak nucleus reaction (blue), as shown in Fig. 7. Such images are like non-CTC, which only respond to red. To analyze this effect in more detail, we believe it is necessary to increase the original number of CTC data and repeat the experiment. In this paper, we proposed a data expansion method that changes the combination of RGB images in CTC, but we also experimented with data expansion by mixing for comparison. The results showed that there were no significant differences between the models compared to the other methods.

Tables III and VI show that the proposed method has better results than the methods of Tsuji et al. In the method using the logical conjunction, since they only used information on whether a cell region is present or not, noise components such as cell debris may be misidentified as CTC. In addition, the method using ANN has a problem in terms of versatility because the features used for identification depend on the designer. However, in the proposed method using the CNN model, the accuracy was improved because the effective features for CTC identification could be automatically selected by learning.

The annotation of the correct data in this study was a manual process by a pathologist. Furthermore, since the number of CTCs identified in this paper is only 148, it is necessary to perform identification experiments with more data and analyze the results for each model, which are future tasks. For this reason, the automatic annotation and balancing of the CTC and normal data must be taken into consideration. Further research is needed to develop software that allows visualization of the results of the detection of cellular regions detected in the original image and the predictions of the model showing the probability of the cell being a CTC.

V. Conclusion

Since there are few image analysis methods that allow quantitative computer analysis for the diagnosis of CTCs in blood, this paper makes a significant contribution by proposing a method that can automatically classify the presence or absence of CTCs. In this paper, we proposed a method for automatic identification of circulating tumor cells from fluorescence microscopy images based on SqueezeNet with SPP. The proposed method was applied to 5040 images for 6 samples and the performance of CTC identification was evaluated. We obtained the results of TPR = 97.30%, FPR = 2.069% and AUC = 0.991 respectively. As shown in Table 6, the proposed deep learning method has a higher discrimination performance than the machine learning method based on image analysis by Tusji *et al.* [5]. To further improve the accuracy, it is necessary to introduce the pre-processing of the input image to CNN, and to conduct the identification experiment with more data and analyze the results. In some experiments using CNN models, CTCs containing multiple nuclei, as shown in Fig. 7, were sometimes incorrectly identified as non-CTCs. For CTC data containing multiple nuclei in the ROI, it is necessary to introduce a process to remove nuclei that exists outside the center. In addition, since the number of CTCs identified in this paper is only 148, it is necessary to conduct identification experiments with a larger number of data and analyze the results. In this study, the selective enhancement filter was used for the segmentation of cellular regions. However, the performance of the filter and comparison with other methods will be necessary. Recently, there have been some classifications of the CTC based on AI [15–20], which are obtained by different devices that are being developed. It is also necessary to evaluate performance in relation to these methods. These are the future tasks.

Conflict of Interest

The authors declare no conflict of interest.

Author Contributions

Kazuki Nakamichi conducted the research and wrote the initial manuscript, and Tohru Kamiya supervised the project, provided suggestions and recommendations along the way. Kazue Yoneda gives medical advice and revised manuscripts. Kouki Tsuji provided suggestions and revised manuscripts. All authors had approved the final version.

References

[1] F. Tanaka *et al*., "Circulating Tumor Cells (CTCs) in lung cancer: Current status and future perspectives," *Lung Cancer: Targets and Therapy*, vol. 1, pp. 77–84, 2010.

[2] Y. Chikaishi *et al*., "EpCAM-independent capture of circulating tumor cells with a 'Universal CTC-chip'," *ONCOLOGY REPORTS*, vol. 37, pp. 77–82, 2017.

[3] K. Yoneda *et al*., "Detection of circulating tumor cells with a novel microfluidic system in malignant pleural mesothelioma," *Cancer Science*, vol. 110, no. 2, pp. 726–733, 2019.

[4] Leica, Products. [Online]. Available: https://www.leica-microsystems.com/products/light-microscopes/p/leica-dmi8-id/
[5] K. Tsuji *et al*., "Detection of circulating tumor cells in fluorescence microscopy images based on ANN classifier," *Mobile Networks and Applications*, 2018. doi: 10.1007/s11036-018-1121-0
[6] Y. Mao *et al*., "A Deep convolutional neural network trained on representative samples for circulating tumor cell detection," in *Proc. 2016 IEEE Winter Conference on Applications of Computer Vision (WACV)*, 2016.
[7] F. N. Iandola *et al*., "SqueezeNet: AlexNet-level accuracy with 50x fewer parameters and <0.5mb model size," arXiv preprint, arXiv:1602.07360, 2016.
[8] K. He *et al*., "Spatial pyramid pooling in deep convolutional networks for visual recognition," in *Proc. European Conference on Computer Vision*, 2014, pp. 346–361.
[9] Q. Li *et al.*, "Selective enhancement filters for nodules, vessels, and airway walls in two- and three-dimensional CT scans," *Medical Physics*, vol. 30, no. 8, pp. 2040–2051, 2003.
[10] T. Lindeberg, "Detection salient blob-like image structures and their scales with a scale-space primal skech: A method for focus-of-attention," *International Journal of Computer Vision*, vol. 11, no. 3, pp. 283–318, 1993.
[11] N. Otsu, "A threshold selection method from gray-level histograms," *IEEE Transactions on Systems, Man, and Cybernetics*, vol. 9, no. 1, pp. 62–66, 1979.
[12] A. Krizhevsky *et al*., "ImageNet classification with deep convolutional neural networks," *Advances in Neural Information Processing Systems*, 2012.
[13] K. He *et al*., "Deep residual learning for image recognition," in *Proc. the IEEE Conference on Computer Vision and Pattern Recognition*, 2016, pp. 770–778.
[14] H. Zhang *et al*., "Mixup: Beyond empirical risk minimization," arXiv preprint, arXiv:1710.09412, 2017.
[15] L. L. Zeune, Y. E. Boink, G. Dalum *et al*., "Deep learning of circulating Tumour cells," *Nature Machine Intelligence*, vol. 2, no. 2, pp. 124–133, 2020.
[16] J.M. Phillip *et al.*, "A robust unsupervised machine-learning method to quantify the morphological heterogeneity of cells and nuclei," *Nature Protocols*, vol. 16, no. 2, pp. 754–774, 2021.
[17] J. Park *et al*., "Microfluidic recapitulation of circulating tumor cell–neutrophil clusters via double spiral channel-induced deterministic encapsulation," *Lab on a Chip*, vol. 21, no. 18, pp. 3483–3497, 2021.
[18] Nakamichi *et al*., "Classification of circulating tumor cells in fluorescence microscopy images based on SqueezeNet," in *Proc. International Conference on Control, Automation and Systems*, 2019, pp. 1042–1045.
[19] B. He *et al*., "A new method for CTC images recognition based on machine learning," *Frontiers in Bioengineering and Biotechnology*, vol. 8, pp. 1–10, 2020.
[20] J. Park *et al*., "Classification of circulating tumor cell clusters by morphological characteristics using convolutional neural network-support vector machine," *Sensors & Actuators: B. Chemical*, vol. 401, pp. 1–9, 2024.